

# Determining Absolute Position Using 3-Axis Magnetometers and the Need for Self-Building World Models

John F. Raquet, Jeremiah A. Shockley, and Kenneth A. Fisher

Air Force Institute of Technology  
AFIT/ENG, 2950 Hobson Way  
WPAFB, OH 45431  
USA

[john.raquet@afit.edu](mailto:john.raquet@afit.edu)

## ABSTRACT

*Magnetic compasses have been used for many years to determine heading for the purpose of dead reckoning. This paper describes a more recently developed method for using 3-axis magnetometers to determine absolute position that is based on taking advantage of local magnetic field variation. The fundamental approach is to compare calibrated 3-axis magnetometer measurements with a previously collected map of the magnetic field (including local variations), and to use this information to estimate the user's current position. This approach has been demonstrated in an indoor environment and in a ground-based vehicle application, showing promise for military navigation in environments in which GPS is not available. Development of a magnetic field map for navigation is one of the challenges of realistic implementation of such an approach, highlighting the need for developing "self-building world models", i.e., using the magnetometer measurement data to continually improve the magnetic field map, possibly in a collaborative manner with multiple sensors. This paper describes the magnetic field modeling approach and gives case studies of its use, and it also describes the more general challenge to develop self-building world models that will be increasingly important as the military attempts to leverage natural signals for navigation in GPS-denied environments.*

## 1.0 INTRODUCTION

Demand is high for navigation solutions in Global Positioning System (GPS) denied environments. There are many different non-GPS approaches that have been considered, and many of these rely on natural signals such as light (vision) or magnetic fields. One challenge with such systems is the need for a reliable map, or "world model", which is required in order to make use of the natural measurements.

This paper first describes this concept of world models, and points out the need to develop self-building world models—that is, world models that are continually constructed as users collect measurements from a particular navigation sensor. The second part of the paper describes a new approach to magnetic field navigation, which is a very good example of the need for a self-building world model.

## 2.0 GENERALIZED NAVIGATION FRAMEWORK

Fundamentally, virtually every navigation algorithm can be viewed through a predict–observe–compare cycle. Consider the flow diagram shown in Figure 1. The "Navigation State" at the lower right represents the user's current navigation state, or all of the information about the user's position, velocity, etc., as well as estimates of that information's quality. This can be thought of as the system's best guess of the user's position as well as how accurate the system thinks the guess is. As depicted in the "Sensor" box on the left, the system takes a measurement or makes an observation which gives some insight into the user's navigation state. For GPS, perhaps the system observes the range to a satellite. The system also uses a model of the real world, depicted with the "World Model" box in the upper right. In the case of GPS, the world model might consist of the locations (orbits) of the GPS satellites.

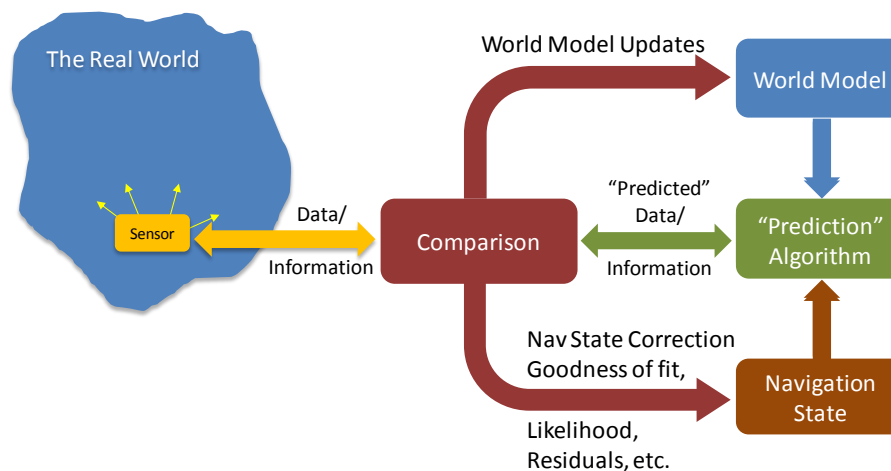


**Figure 1: General Navigation Algorithm—virtually every navigation system follows this process.**

During the predict phase, the prediction algorithm determines what the system expects to observe based upon the world model and the current navigation state, annotated as the “Prediction Algorithm” box in Figure 1. During the observe phase, the system receives a noise-corrupted measurement from the real world. During the compare phase, the predicted measurement is compared to the actual measurement. Any discrepancies are used to improve the navigation state and possibly the model of the world.

Consider a simplified example in which a user attempts to determine the distance to a wall. Perhaps the user predicts the distance to the wall is about 30 feet based upon mere eyesight to judge the distance. (The navigation state is 30 feet with much uncertainty.) Then, suppose a precise laser range finder is used to measure, or observe, the distance as 31.2 feet. Next, the prediction is compared to the observation. The user quickly dismisses the prediction and trusts the observation, because the user observation was viewed as being a more reliable estimate of distance than the prediction. Likewise, examples could be drawn which highlight the prediction heavily outweighing an observation. (Perhaps if a child provided information about why the sky is blue to a meteorologist, the meteorologist would trust his own information over the new information.)

The most interesting applications involve a blending of the prediction with the observation. Typical GPS applications use a Kalman filter [1] to perform the predict–observe–compare cycle. The world model consists of GPS satellite locations. Based upon some prior information, the receiver predicts the user’s location. The observations might consist of ranges to each satellite in view. These observations are compared to a prediction of what the ranges should be based upon the receiver’s estimate of position (and assumed knowledge of the world). The system conducts a blended comparison based upon the relative quality of the predicted navigation state and the observations.

## 2.1 World Model Updates

In Figure 1, the arrow labeled “world model updates” indicates that the world model can be changed based upon the measurements that have been taken. Some navigation systems, particularly those which are designed and deployed specifically for navigation, do not require the end user of the system to be involved in this part of the process. For example, in GPS, the “world model” consists of information about the satellite orbits (ephemeris), the satellite clock errors, and details that are given in the signal specification (frequency, chipping rate, etc.). The GPS system uses its own receiver network on the ground to estimate satellite orbits and clock errors and to monitor the signals coming from space, and measurements from this network are used to continually update the GPS “world model”. As a result, the user simply obtains the most recent

ephemeris and satellite clock terms and uses them for positioning. In this way, the user is completely uninvolved in the updating of the world model, which is helpful, because it greatly reduces the complexity of the system for the user.

## 2.2 Need for Self-Building World Models

Unlike man-made signals, natural signals do not generally have a dedicated part of the system that is continually updating a concise “world model” which describes how sensed measurements relate to the real world. Table 1 gives some examples of natural signals and the type of information in the world model that is needed to use these signals for navigation.

<b>Natural Signal</b>	<b>“World Model” Information Needed for Positioning</b>
Earth’s magnetic field	Map of magnetic field variations (described later in this paper)
Gravity	Model of the earth’s gravitational field
Lightning	Location and timing of lightning strikes, propagation parameters
Light (received by cameras)	Model of what the world “looks like” as a function of position/orientation. This can include either features or full 3-D models with texture.
X-Ray pulsars	Timing and signal characteristics of x-ray signal, direction of arrival
Sound	Knowledge of what sounds are present at various locations/times

**Table 1: World model information required to use various natural signals for navigation.**

When examining the natural signals given in Table 1, it is evident that some of these signals are fairly consistent (such as gravity), and some of them can change significantly over time (such as light). As a result, there is not a world model that can simply be downloaded and used within a navigation system. (An exception to this may be gravity, which has been modelled to a high degree of fidelity, partly due to the fact that it doesn’t change in an unpredictable manner like the other natural signals do).

For signals that change significantly over time or for which there is no existing high-fidelity world model, the only practical method for developing the world model is to have it self-build—that is, to continually update the world model using the measurements that are being used for navigation. A good example of this is human navigation using vision. If a person moves to a new city that they’ve never visited before, everything that they see for the first time will initially be used to build their world model of their new city. However, as time passes and they revisit various locations, their growing world model will enable them to know exactly where they are as they observe with their eyes, and compare those observations with their self-building world model in a manner described in Figure 1.

Another good example of the need for a self-building world model is navigation using variations in the earth’s magnetic field. Such variations are highly complex and can change over time, so it is not practical to have a large measurement campaign to determine the full three-dimensional magnetic field everywhere in the world. However, it would be feasible for people and/or vehicles who are navigating to collect magnetic field information as they go and use it both for their own navigation and also use it for developing a continually growing magnetic field world model. In this approach, the ability to share information between various sensors is of high value. If a user is able to take advantage of a world model developed by hundreds or thousands (or even millions!) of other users, their ability to navigate will be greatly improved over a situation where they can rely only on their own measurements. This ability to collaborate in the development of a world model is one advantage that we have over natural navigators (humans and animals)—it is generally easier to share information between sensors than it is to share information between humans or animals.

### **3.0 MAGNETIC FIELD NAVIGATION**

A new form of magnetic field-based navigation provides an excellent example of the need for self-building world models, and the rest of this paper will focus on this approach. While using Earth's magnetic field for navigation is certainly not a new concept, the use of specific magnetic field information mapped to a geographic position is growing in popularity. Wilson et. al., propose using magnetic field variations over a large area to navigate in an aircraft using US Geological Survey magnetic field maps. The algorithm uses the magnetic field information combined with an aircraft dead-reckoning navigation system to determine the aircraft position [2]. Flight test results compare the dead-reckoning solution with the magnetically aided navigation solution to demonstrate the navigation solution improvement, but the position accuracy observed was on the order of 2.5 km. Storms applied a terrain navigation algorithm to the indoor magnetic field environment and achieved sub-meter accuracy positioning results [3,4]. Using real measurements the maximum error is 0.6 meters. This fundamental work establishes the use of unique three-axis magnetic field measurements as navigable features and demonstrates effective use of the information. Judd and Vu tackled an indoor pedestrian navigation problem, noting interesting correlation in three-axis magnetometer measurements in the indoor environment [5]. While attempting to correct heading estimation indoors, the magnetic field along the route exhibits distinct "fingerprints" at unique locations along the route [5]. The resulting fingerprints allow correlation of previous magnetic field data with measurements during a new route to determine if a specific location is reached.

This paper describes the use of magnetic field variation for determining position of a ground vehicle. First, the concept of operation will be described, followed by a description of how a position can be determined using magnetic field variations. Finally, examples of this approach will be given for a number of tests that were conducted at the Air Force Institute of Technology and surrounding areas.

#### **3.1 Concept of Operation**

Initially, a three-axis magnetometer is mounted in a convenient location in a vehicle and aligned with the body frame, careful to avoid large emitters of electromagnetic interference (EMI). Next, a calibration should be performed in order to mitigate the magnetic field distortion caused by the vehicle. As a part of this calibration, the characteristics of the measurement noise are determined. These noises are needed in order to properly use the data. At this point the system is set up and ready to go.

After initial setup, there are two main stages to this approach—the mapping stage, and the navigation stage. In the mapping stage, data is collected from three-axis magnetic field information from the magnetometer at times when the vehicle position is known (such as when GPS is available). This data is stored along with the corresponding positions, creating a "world-model" or map of the three dimensional magnetic field over the roads that have been traversed during this stage.

In the navigation stage, the vehicle is driving over roads that have been previously mapped, and the desire is to determine position using only the measurements from the magnetometer. This is accomplished by taking the raw measurements, applying the previously-determined calibration, and then comparing them to the map. This is accomplished in our approach by using a Gaussian likelihood, which assigns a higher likelihood value to places on the map which closely match the collected measurements. Then position determination can be performed by using the likelihood values in one of three ways:

- 1) **Maximum Likelihood (ML)**--Selecting the position on the map which has the maximum likelihood and using that as the position measurement
- 2) **Maximum Likelihood Ratio (MLR)**—A variation of the maximum likelihood approach in which only maximum likelihoods that sufficiently stand out from all nearby likelihoods is considered a valid position measurement

- 3) **Particle Filter (PF)**—Position is estimated using a particle filter, in which the likelihood values are used in the update stage for the particles.

Figure 1 depicts the stages described in this concept of operation. Note that this approach could be an example of a self-building world model, in that the same sensors used for navigation (magnetometers in this case) are also being used for developing the world model.

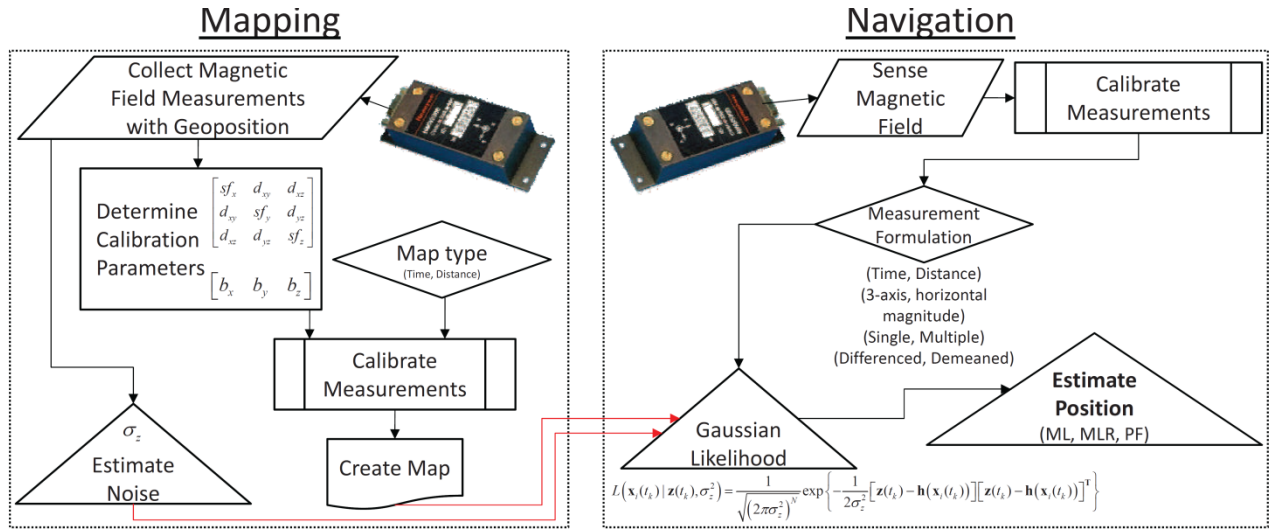


**Figure 1: Concept of operation of magnetic field navigation system.**

### 3.2 Position Measurement Generation

In this paper, likelihood methods are used for position estimation, but are not the only method which could be used. The generalized multivariate Gaussian likelihood function from Maybeck [1] is and provides a scalar likelihood value for each magnetic field map location  $\mathbf{x}$ :

$$L(\mathbf{x}|\mathbf{z}, \mathbf{P}) = \beta \exp\left\{-\frac{1}{2}[\mathbf{z} - \hat{\mathbf{z}}]\mathbf{P}^{-1}[\mathbf{z} - \hat{\mathbf{z}}]^T\right\} \quad (1)$$

$$\beta = 1/\sqrt{(2\pi)^N |\mathbf{P}|}$$

The  $\beta$  term outside the exponential represents a scaling factor conditioned on  $\mathbf{P}$ , which can lead to a condition known as  $\beta$  dominance [6].  $\mathbf{P}$  is the measurement covariance matrix.  $N$  indicates the number of measurements in the measurement vector  $\mathbf{z}$ . The incoming measurements  $\mathbf{z}$  provide the most recent measurement available, while  $\hat{\mathbf{z}}$  represents the predicted magnetic field for any given point in the map. If the magnetometer measurement matched a measurement contained in the magnetic field map perfectly, the likelihood would be very high. Similarly, a magnetometer measurement very different from those contained in the magnetic field map would have a likelihood approaching zero. Figure 2 depicts a sample set of likelihoods at a single epoch, where the  $\beta$  term has been removed to normalize the plot. The sample set of likelihoods at a single epoch shows the relationship between a single measurement and the entire magnetic field map. The likelihood is near zero for a large portion of the map, but depicts several peaks which are possible locations based on the magnetometer measurement. The peaks are formed as the magnetometer measurement approaches a potential match in the magnetic field map.

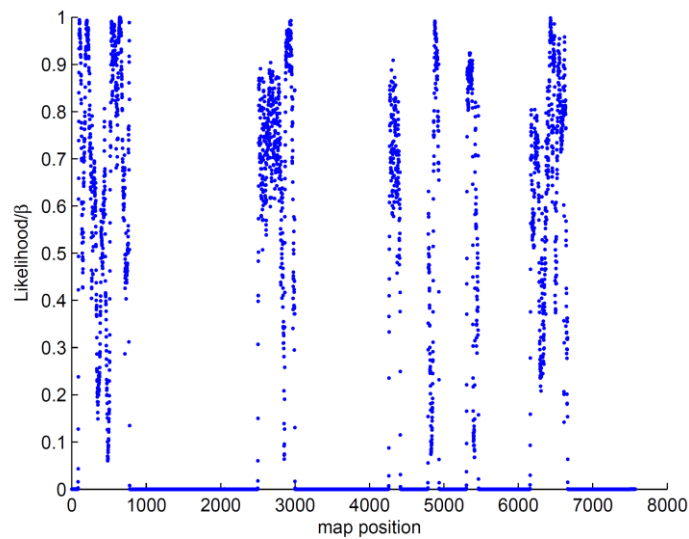


Figure 2: A sample set of likelihoods at a single epoch, as a function of position on the map. The  $\beta$  term has been removed to normalize the plot.

The likelihood map in Figure 3 shows the likelihood of each point on the magnetic field map for each epoch. The color intensity shows the relative difference between low likelihoods (near zero) and high likelihoods (near the maximum). The information this graphic conveys is that there are definite areas with sufficient measurements to perform likelihood matching and obtain a position estimate. If the entire graphic were solid blue (low likelihood), none of the magnetometer measurements correlated well with the magnetic field map, or there was insufficient change in the magnetometer measurements and the magnetic field map to differentiate between positions. Perturbations, or features, provide unique areas and the more unique the feature, the fewer locations on the likelihood map will be highlighted. But by and large, the areas emphasized in the likelihood map are due to similar heading characteristics. Although not explicitly calculated, the horizontal axes of the magnetometer are a function of heading. As a result, the likelihood of similar headings will be higher than magnetometer measurements from different headings.

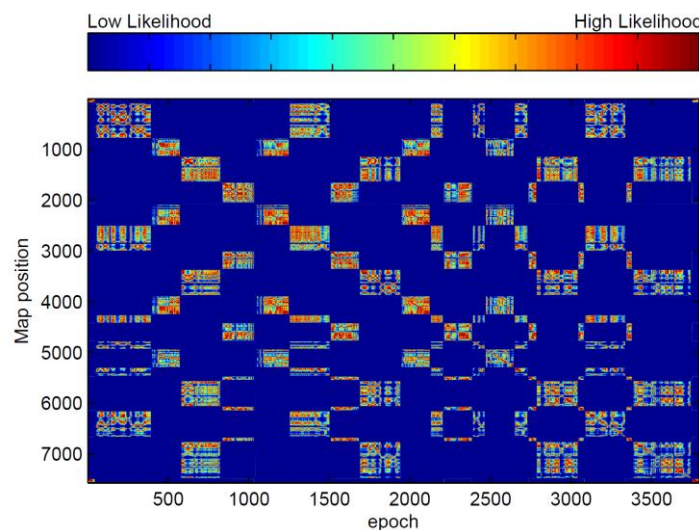


Figure 3: Likelihood for all map positions as a function of epoch number.

The magnetic field map is composed of numerous positions defined by their fairly unique three-axis magnetometer measurements and restricted to roads. An incoming magnetometer measurement can easily be compared to every magnetic field map measurement and the resulting set of likelihoods used to determine the most likely position on the map. The following sections detail the maximum likelihood (ML) and maximum likelihood ratio (MLR) approaches for generating a position measurement directly from the likelihood values.

### 3.2.1 Maximum Likelihood (ML)

Using the maximum of the likelihoods from Equation 1 provided a simple and effective way to determine the best magnetic field map location according to the magnetometer measurement. However, due to the nature of the magnetometer measurements, the maximum likelihood value is not always correct. Another look at the sample set of likelihoods for a single epoch depicted in Figure 3 easily casts doubt that simply picking the maximum likelihood will result in the correct magnetic field map location. The maximum likelihood also provides a straightforward baseline indicator for comparing other techniques.

### 3.2.2 Maximum Likelihood Ratio (MLR)

Since using the maximum likelihood alone does not always produce the correct location via the magnetic field map, a technique to help determine if the maximum likelihood is correct proved useful. When multiple likelihood peaks are present, the maximum likelihood is divided by the second highest likelihood a specified minimum distance from the position of the maximum likelihood (e.g., 20m) to form the maximum likelihood ratio. If the ratio exceeds some value (e.g., 2) then the maximum likelihood is sufficiently unique to provide a location estimate. However if the ratio does not exceed the threshold, no location estimate is reported, meaning some epochs will be deemed insufficient to provide an estimate. Therefore the MLR sacrifices availability in order to increase accuracy of the position estimate. The motivation for this approach stems from observation of the set of likelihoods as magnetometer measurements are compared to the magnetic field map. As each incoming magnetometer measurement gets closer in position to a magnetic field map location that correlates well, the set of likelihoods form a peak. If the magnetometer measurement and magnetic field map correlation is truly unique, a single peak is formed. However, multiple peaks are often formed indicating other possible locations. The maximum likelihood ratio provides a method to determine if the second highest peak is sufficiently different in position and substantially lower in likelihood to assert that the maximum likelihood is correct.

Clearly, the ratio and minimum distance values play an important part in the results provided by the MLR. A very short minimum distance will only allow sharper peaks which express a close match between the magnetometer measurement and a particular magnetic field map location. This may eliminate areas where the peak is wide due to the magnetometer measurement being equally likely for several epochs (common on roadways). While a larger minimum distance would alleviate this symptom, it also may reduce the accuracy of the match, since the maximum likelihood may be at any location within the minimum distance due to several high likelihood values in succession. The ratio also affects the quality of the match. As the value of the ratio increases, the vertical distance between the maximum likelihood peak and the next peak increases and expresses the uniqueness of the peak. However, too high a ratio will reduce matches to only the very unique. On the other hand, a ratio that is too low will not allow sufficient distinction between peaks of nearly the same height, and reduce discernment that the maximum likelihood is the correct peak. Overall, a high ratio combined with a short minimum distance will identify unique peaks higher than all other peaks. However, the cost for the increase in quality is the number of available matches between a magnetometer measurement and the magnetic field map. Conversely, a lower ratio and longer minimum distance will allow more matches, but with less accuracy. The ratio and minimum distance values for the MLR were selected from empirical analysis.

### 3.3 Particle Filter Approach

In contrast with the methods from 3.2 which generate a single position measurement directly from the likelihood values, a particle filter can be used to incorporate the information from the likelihoods as measurement updates. A particle filter is a technique for implementing a recursive Bayesian filter by Monte-Carlo methods [7]. The particle filter attempts to represent the required posterior density function (PDF) using a set of random samples with associated weights. The estimates are then determined from the samples and weights. Each sample can be thought of as an individual state estimate, with an importance conveyed by the associated weight. In terms of magnetic field navigation, the particle filter allows the multiple estimates to represent possible locations in the magnetic field map, and the incoming measurements help convey the importance a particular estimated location should possess. As evidenced by Figure 2, the comparison of an incoming magnetometer measurement to the magnetic field map highlights the possibility of multiple locations. The particle filter yields the ability to use that information, as well as a dynamics model based on the vehicle characteristics, to provide position estimates for navigation. The navigation solution comparison will use the same particle filter and modify the measurement update portion. This allows comparison using both a position estimate as the measurement update as well as direct incorporation of the three-axis magnetometer measurements. A general overview of particle filtering can be found in [1] and [8]. Overall, the MagNavigate particle filter consists of propagation, a road penalization update, and a measurement update (using either estimated position or direct magnetometer measurements). Each of these will be described in the sections that follow.

#### 3.3.1 Propagation

Particle propagation is performed using a first-order Gauss-Markov acceleration model [1], with a time constant of 2 seconds and a standard deviation is  $5 \text{ m/s}^2$ , which is reasonable for a ground vehicle including starting and stopping. Particles propagate freely based on the dynamics model, but are penalized based on their distance from the closest known road.

#### 3.3.2 Road Penalization Update

Since the magnetic field maps are limited to existing roads, penalizing particles far from any road in the magnetic field map is reasonable. Rather than arbitrarily remove particles, the Gaussian likelihood from Equation 1 was used to penalize particles based on the distance from any location in the magnetic field map. This update occurs regardless of any measurement update and allows particles on the road to receive a higher likelihood than particles not on the road. This allows viable particles to continue while penalizing particles that are not viable (i.e., not on ANY road in the magnetic field map). The set of likelihoods for the particle collection is then used to update the associated weights.

#### 3.3.3 Measurement Update

This research investigated two different types of updates: 1) a position update in which the magnetometer measurements were converted to a position via a likelihood technique (ML or MLR), and then applied in the filter, and 2) a magnetometer update in which the actual magnetometer measurements were directly used to update the filter. Each of these will be described in the paragraphs that follow.

The position update is expressed as

$$\mathbf{z} = [p_e \ p_n] \quad (2)$$

where the east position  $p_e$  and north position  $p_n$  are in the local level frame. The position update obtains a position estimate using the aforementioned likelihood techniques. Since  $\mathbf{z}$  is a position,  $\hat{\mathbf{z}}$  is based on the position information in the magnetic field map to determine the likelihood values.



In contrast, the magnetometer update uses the three-axis measurements directly from the magnetometer along with Equation 1. The magnetometer update is expressed as

$$\mathbf{z} = [B_x \ B_y \ B_z] \tag{3}$$

where  $B_x$ ,  $B_y$ , and  $B_z$  are the observed three-axis magnetometer measurements in the x, y, and z-axis, respectively. In this case,  $\hat{\mathbf{z}}$  is based on the three-axis magnetic field information contained in the magnetic field map to obtain the likelihood values.

Particle resampling was accomplished after measurement incorporation in order to eliminate particles with low likelihood and increases the number of particles in high likelihood areas without changing the PDF. The resampling method used for this research was sequential importance resampling [8].

### 3.3.4 Particle Filter Implementation Example

Figure 4 illustrates the entire particle filter (propagation, road penalization, and measurement update), the upper left of Figure 5 shows the initial random particle collection (red dots) before any distance based restriction is applied in a suburban neighborhood scenario (thin black line). The weighted particle mean (blue asterisk, which overlays the black dot) conveys the current position estimate. The uncertainty (dashed blue line) is calculated as in Van der Merwe [9]. After the map-matching likelihood update is applied to the particle weights and resampled, the particles near the road have been kept as well new particles spawned near the same locations, seen in the upper right of Figure 4. As propagation continues, if no measurement updates are applied the particles continue along the map. The lower left depicts propagation after 100 cycles when no magnetometer measurement updates are applied. The vehicle track (thick black line) conveys how far the position should have moved. In contrast, the lower right shows the particle collection after 100 propagation cycles when regular measurement updates are applied, conveying movement along the road. The navigation solution (MagNavigate green dots) highlights the weighted particle mean, slightly ahead of the vehicle track. The outcome is a navigation solution detailing the position of the vehicle based solely on the magnetometer measurements and magnetic field map.

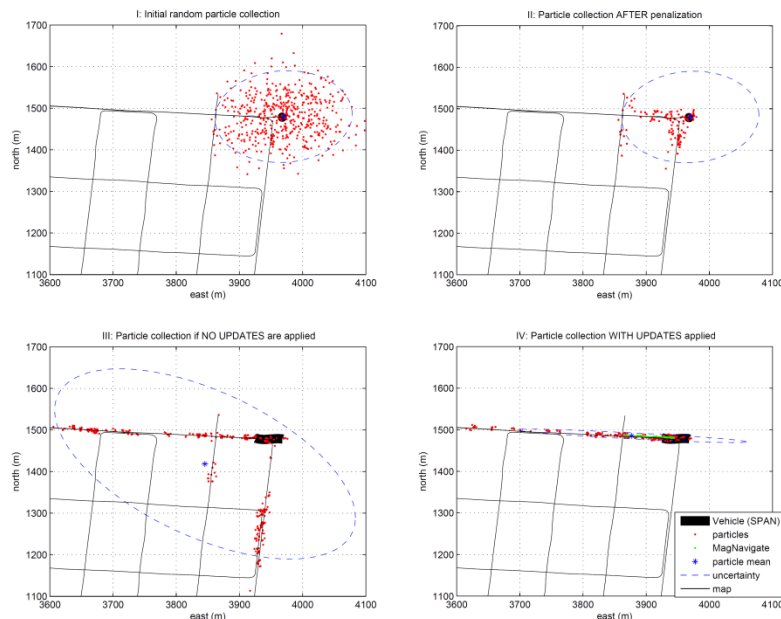


**Figure 4: Example of particle filter propagation and update.**

### 3.4 Field Test

A field test was conducted to test the feasibility of this kind of magnetic field navigation approach. Three different types of vehicles were used—a 2004 Chevrolet Avalanche truck, a 2003 Pontiac Aztek sports utility vehicle (SUV), and a 2005 Nissan Altima car. Each platform represents a different vehicle type in order to demonstrate portability across vehicles. A Honeywell HMR2300 magnetometer was mounted in each vehicle on a level surface and aligned with the body frame as much as possible. Care was taken during placement to avoid powerful emitters of magnetic fields to mitigate EMI. However, the magnetometer was always mounted inside the cargo or passenger areas of the vehicle with no special extensions to distance the magnetometer from the vehicle. Therefore EMI from the engine, turn indicators, and other sources is present under typical operating conditions. A NovAtel SPAN GPS receiver collected position information for mapping and as a truth reference. (Only the GPS solution from SPAN was used in this research, so any GPS receiver would have been adequate). An example of the installation is shown in Figure 5. The magnetometer was calibrated by driving the vehicle in concentric circles and using a modified ellipsoid calibration method [10], with a measurement collection rate of 50Hz.

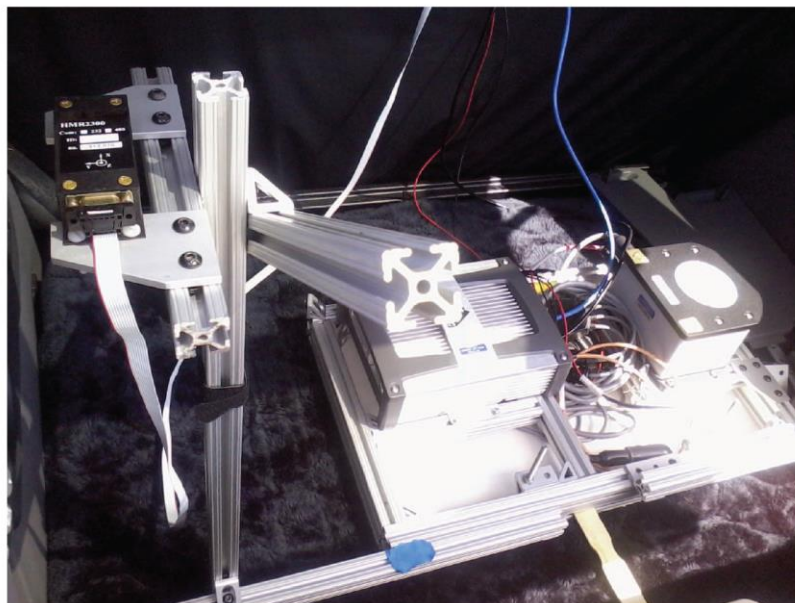


**Figure 5: HMR2300 and SPAN mounted in the SUV cargo compartment.**

For the navigation results presented in this paper, the position coordinates were converted to a local level frame of east, north and up (ENU) using a coordinate transformation. All roadways were traversed under normal conditions (i.e., speed limits, stop signs, traffic lights, passing vehicles, pedestrians). The magnetometer axes were aligned with the body frame of the vehicle.

#### 3.4.1 Test Route Descriptions

Figure 6 displays the three different road environments used in this test. The upper left map in Figure 6 shows the initial route and consists of a fairly benign environment around the Air Force Institute of Technology (AFIT). The upper right map covers a suburban neighborhood and allows investigation of the ability to discern position on parallel roads in a similar environment. The bottom map covers a large area and shows the relative locations of the suburban neighborhood and AFIT map areas. The colors are only used to highlight the route and possess no other meaning.

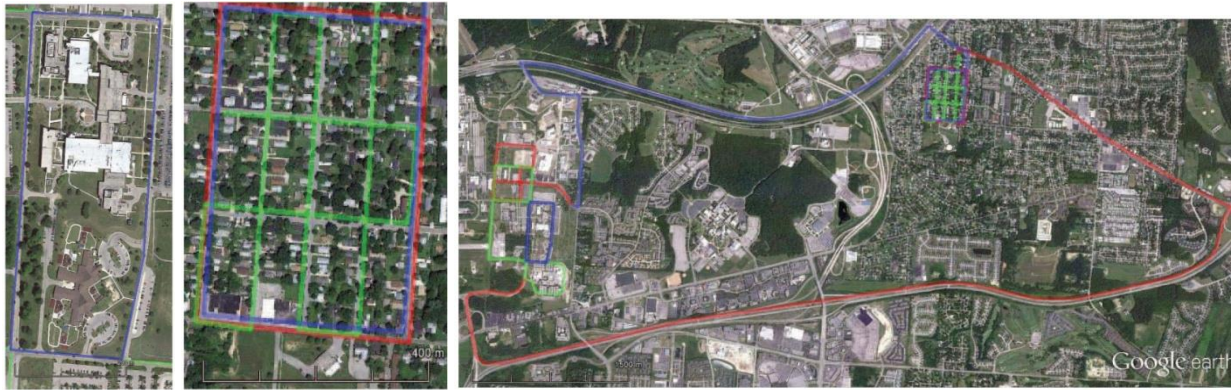


**Figure 6: Three test routes described in this paper—AFIT (left), neighbourhood (center), and large area (right).**

### 3.4.1 AFIT Route Test Results

The left side of Figure 7 shows the GPS-based vehicle track (thick black line) and the MagNavigate filter solution (green dots that appear like a line). Each green dot represents the weighted particle mean. While the system appears to track quite well, Figure 7 does not convey the “along-track” error in the system. The corresponding position error plot on the right side of Figure 7 displays the east, north, and horizontal position errors versus time for the same AFIT test.

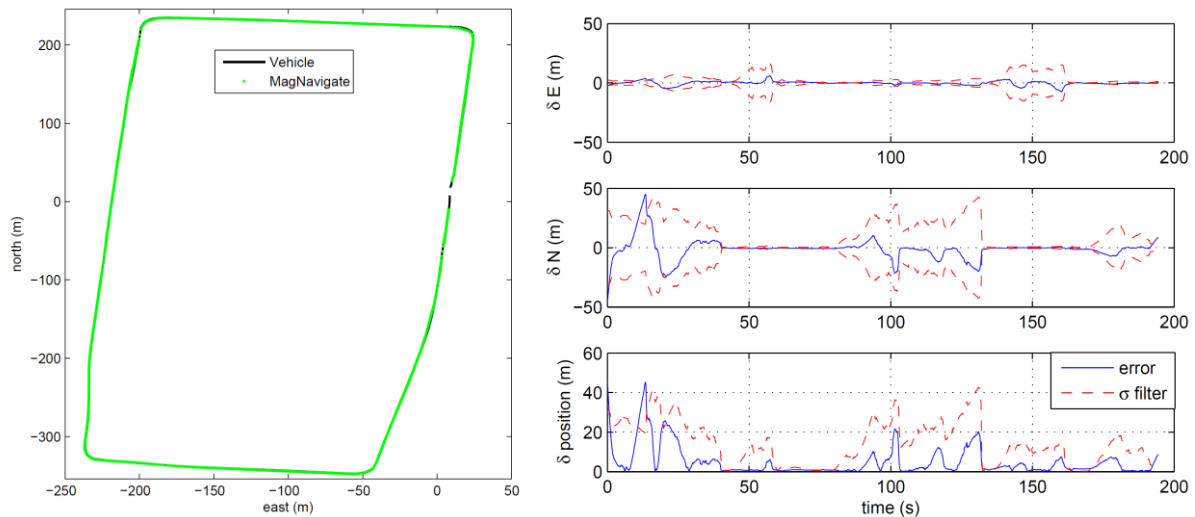


**Figure 7: AFIT route test results.**

The right side of figure 7 consists mostly of along-track error, which is why the map plot on the left looks good. When there are not unique magnetometer measurements, the error and associated uncertainty tend to increase in the along-track direction. The primary reason for this is that the road penalization update described previously keeps the particles near the road.

Examining many plots like Figure 7 for every combination of navigation solution would be cumbersome. Instead, the results have been grouped in Figure 8 to show performance statistics for comparison of the overall position errors by using the maximum position error and the horizontal root-mean-square (RMS) position error. Figure 8 includes cross-vehicle cases using the AFIT map. The notation T-S indicates the

Truck-SUV case and indicates that the truck navigated using a magnetic field map created in the SUV. Additionally, the three different measurement types are included—ML, MLR, and direct magnetometer update.

The maximum likelihood displays the largest max error, yet displays RMS errors slightly higher than the MLR and magnetometer update. The maximum likelihood as the position update in the particle filter delivers a fairly consistent level of navigation. By comparison, the MLR delivers one case of improved performance (T-S), along with a similar performance for the C-S and worse performance for the T-C case. The results are inconsistent due to factors such as measurement availability and propagation error. Lastly, the direct incorporation of measurements for the magnetometer update appeared fairly consistent while delivering some of the best RMS values. Given this assessment, the magnetometer update is used for the remaining results in this paper. However, this does not discount the value of the position update. While this direct measurement update implementation yields a slight edge in performance using the magnetometer update, the same cannot be assumed for every filter implementation. Additionally, multiple sensor implementations may benefit from the adjustable performance allowed by the MLR as a position update rather than attempting incorporation of the magnetometer update [10].

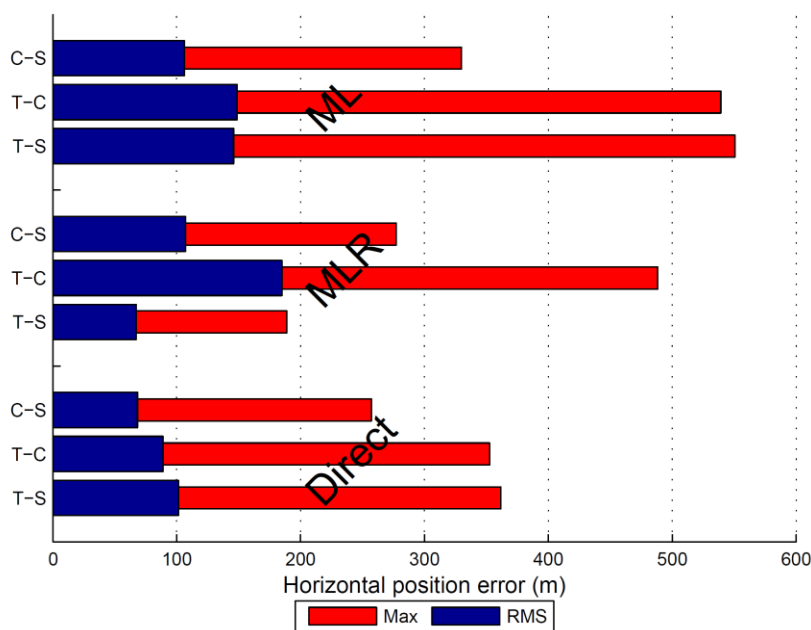


**Figure 8: Horizontal navigation performance comparing the different measurement updates and cross-vehicle cases—AFIT route.**

### 3.4.2 Neighborhood Route Test Results

Figure 9 provides an example of navigation filter performance using the suburban neighborhood map. This neighborhood route was chosen because it is riddled with similar features and roadways, which dilutes the uniqueness of magnetometer measurements in the magnetic field map, increasing the possibility of selecting the wrong road during navigation. In the suburban neighborhood case, propagation error is evident in both figures. A few areas in the left side of Figure 9 display quick traversal over a section of road, evident by the sparseness in the navigation solution. If the particle filter receives poor measurements, especially after stopping, the navigation solution may fall behind the actual vehicle track. Once a very good measurement is observed, the navigation solution quickly catches up to the correct position, exhibiting the sudden reduction in error after a long propagation error. Examining the error plot in Figure 9 reveals that the environment is

challenging for the particle filter. The horizontal position error plot depicts rampant propagation error followed by small periods of nearly no error. This is common for the suburban neighborhood since many locations in the magnetic field map exhibit similar magnetometer measurements which leads to growing uncertainty in the particle filter. Fortunately, unique magnetometer measurements are received often enough that the particle filter converges on a position and continues navigation.

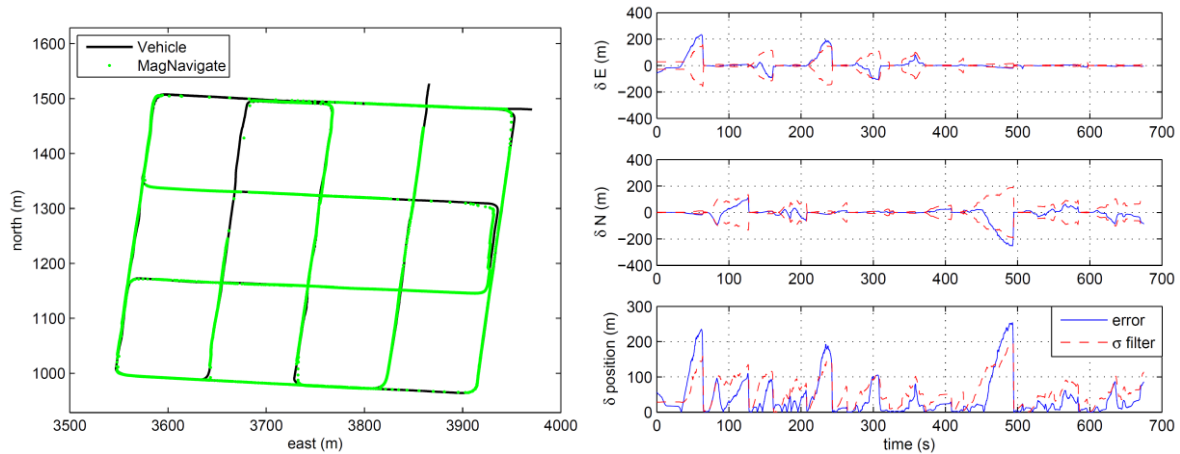


**Figure 9: Neighborhood Route Test Results**

### 3.4.3 Large Area Route Test Results

As seen in Figure 6, the large map contains stretches of highway and roads without significant structure to create magnetic features. This presents an environment with fewer features over long periods, resulting in less useful magnetic field information. Figure 10 depicts the navigation solution and corresponding error plot for the large area route.

The large area route contains a few problem areas, which is to be expected. The portions that do not track well are largely the result of the lack of significant variation in the magnetometer measurements. The highly noticeable track error on the northern portion of the map actually shows the navigation solution is no longer on the road. In this particular case, the particles have propagated all along this stretch of road. The navigation solution (the weighted particle mean) lies just north of the true trajectory since particles to the east and west contained enough weighting to cause the weighted particle mean to be off the road, even though all the particles are on the road.

Further to the right near 4000m east and 1900m north the particles have largely split into two groups, with the first group maintaining the correct navigation solution. However, examining the error plot in Figure 11 near 900 seconds highlights a spike in all three error plots. For this short series of epochs the incorrect group of particles momentarily gains enough weight to shift the navigation solution. Within a few measurement updates, the correct group of particles regains the weight to shift the navigation solution back where it should be and continue on the correct path. For those few epochs, the magnetometer measurement update matched the wrong location in the magnetic field map so well that the navigation solution is actually shifted approximately 1 kilometer (km). This update error is quite different than the typical propagation errors which are experienced the majority of the time.

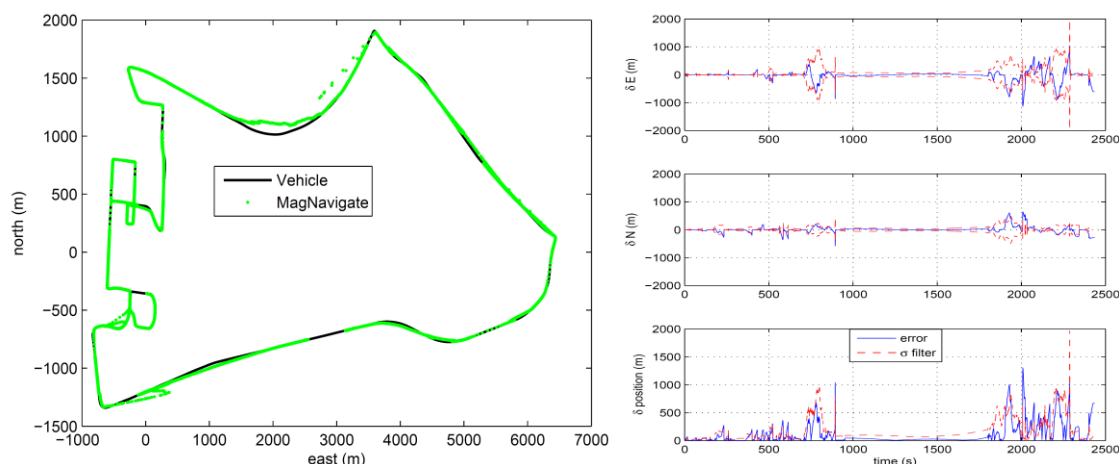


Figure 10: Large Area Route Test Results

## 4.0 CONCLUSION

This paper demonstrates that ground vehicle navigation using magnetic field variations delivers road-level navigation in differing environments. Repeatable magnetic field maps provide the infrastructure to utilize incoming magnetometer measurements and calculate the likelihoods. The likelihood techniques enabled position measurement generation, not only useful for standalone magnetic field navigation, but easily implementable in other navigation systems with the ability to accept a position input for correction. The MagNavigate particle filter incorporates the knowledge from either measurement update method, as well as the propagated particles limited to the road, to determine an effective navigation solution. Navigation using magnetic field variation capitalizes on the rich information and global prevalence of the Earth's magnetic field to provide a self-contained navigation solution.

This magnetic field navigation approach also serves as an example of the need for self-building world models. While this test involved returning to routes previously mapped out for this purpose, such an approach may not always be feasible, especially for military applications. Therefore, there is a need to develop methods to have a self-building world model in which the magnetic field map is being built up by those who have a good navigation solution at the same time it is being used by those who do not, and need to use the magnetometer measurements for positioning. Both world model building and navigation are performed using the same magnetometers.

## 5.0 DISCLAIMER

The views expressed in this paper are those of the author and do not reflect the official policy or position of the United States Air Force, Department of Defense, or the United States Government.

## 5.0 REFERENCES

- [1] Maybeck, P., *Stochastic Models, Estimation, and Control (Vol 1)*, Navtech Book and Software Store, 1994.
- [2] Wilson, J., R. Kline-Schoder, M. Kenton, P. Sorensen, and O. Clavier, "Passive Navigation Using Local Magnetic Field Variations," *Institute of Navigation International Technical Meeting*, Monterey, CA, Jan 2006.

- [3] Storms, W., *Magnetic Field Aided Indoor Navigation*, Master's thesis, Air Force Institute of Technology, March 2009.
- [4] Storms, W. and J. Raquet, "Magnetic Field Aided Vehicle Tracking," *Proceedings of ION GNSS-2009*, Savannah, GA, Sep 2009.
- [5] Judd, T., and T. Vu, "Use of a New Pedometric Dead Reckoning Module in GPS Denied Environments," *Proceedings of IEEE Position, Location and Navigation Symposium (PLANS)*, Monterey, CA, May 2008.
- [6] Clark, C., *Multiple Model Adaptive Estimation and Control Redistribution Performance on the Vista F-16 During Partial Actuator Impairments*, Master's thesis, Air Force Institute of Technology, March 1997.
- [7] Arulampalam, S., S. Maskell, N. Gordon, and T. Clapp, "A Tutorial on Particle Filters for Online Nonlinear/Non-Gaussian Bayesian Tracking," *IEEE Trans. on Signal Processing*, Vol. 50, pp. 174-188, 2002.
- [8] Ristic, B., S. Arulampalam, and N. Gordon, *Beyond the Kalman Filter: Particle Filters for Tracking Applications*, Artech House, Boston, MA, 2004.
- [9] Van der Merwe, R., A. Doucet, N. de Freitas, and E. Wan, *Unscented Particle Filter*, Technical Report CUED/F-INFENG/TR 380, Cambridge University Engineering Department, Cambridge CB2 1PZ, England, 2000.
- [10] Shockley, J. *Ground Vehicle Navigation Using Magnetic Field Variation*. Ph.D. thesis, Air Force Institute of Technology, Sep 2012.

